2067-17

**Joint ICTP/IAEA Workshop on Irradiation-induced Embrittlement of
Pressure Vessel Steels**

23 - 27 November 2009

**Modeling and Simulation to Reveal Radiation
Damage Mechanismsin RPV Steels**

Randy K. Nanstad

*Oak Ridge National Laboratory
U.S.A.*

Randy K. Nanstad

Leader, Nuclear Materials Science and Technology Group

Materials Science and Technology Division
Oak Ridge National Laboratory
Oak Ridge, Tennessee, USA

Contributions from: Roger Stoller, Yuri Osetsky

Modeling and Simulation to Reveal Radiation Damage Mechanisms in RPV Steels

Joint ICTP/IAEA Workshop on Effects of Mechanical Properties and Mechanisms Governing the Irradiation-induced Embrittlement of Pressure Vessel Steels

Abdus Salam International Centre for Theoretical Physics (ICTP)
Trieste, Italy 23-27 November 2009

Materials Science and Technology Division
Oak Ridge National Laboratory

ornl

UT-BATTELLE

D0000998

Why do we care about radiation damage in structural materials - What is the impact?

Desirable material properties: strength, ductility, toughness, dimensional stability, are all largely determined by the nature of their defect structure

- grain size, other internal interfaces
- dislocation density
- size and density of second phase precipitates

○ vacancy
● interstitial

Irradiation with energetic particles leads to atomic displacements

Incoming particle

Primary knock-on atom - PKA

- neutron exposure can expressed in terms of particle fluence ($\#/m^2$) or a dose unit that accounts for atomic displacements per atom - **dpa**
- lifetime component exposures are in the range of ~0.01 to more than 100 dpa
- cumulative impact of atomic displacements: radiation-induced evolution of pre-existing microstructure and the formation of new defect structure

ornl

R. E. Stoller, ORNL
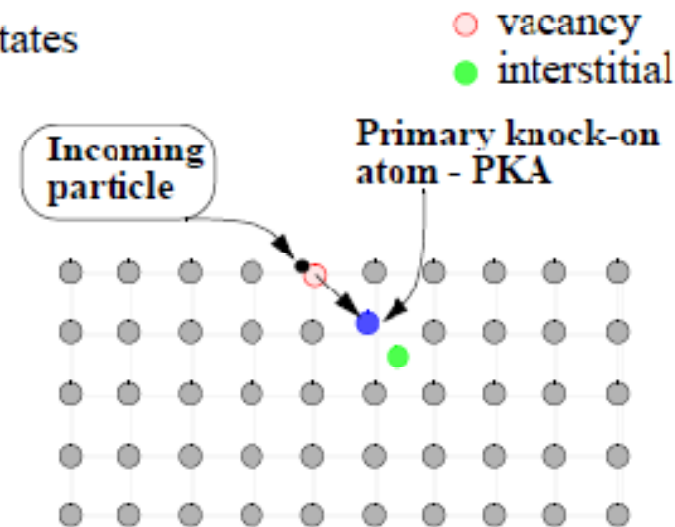
Why do we care about __modeling__ radiation damage in structural materials?

Although irradiation experiments can not be replaced by modeling alone, a purely experimental approach to understanding the effects of irradiation is also not practicable

- costs for design and execution of reactor irradiations
- costs of post-irradiation examination of radioactive materials
- declining facilities for both irradiation and examination
- combinatorial problem: broad range of materials, phenomena, and irradiation conditions - coolants, temperature, loading conditions, dose rate, dose

Recent advances in computational hardware, computational science, ... make it more feasible than ever to aggressively attack this challenge

- e.g. April 2004 SC-NE Workshop on Advanced Computational Materials Science: Application to Fusion and Generation IV Fission Reactors, report at: http://www.csm.ornl.gov/meetings/SCNEworkshop/DC-index.html

ornl

R. E. Stoller, ORNL

ornl

UT-BATTELLE *D0000998* 3

Schematic diagram: relevant phenomena and computational methods

Phenomena

void swelling, hardening, embrittlement, creep, stress corrosion cracking, ...

defect and solute migration and clustering

single displacement cascade

multiple cascades, cascade overlap

collisional phase

annealing phase

defect/solute diffusion

microstructure evolution

quenching

mechanical property changes

10^{-14} s 10^{-11} s 10^{-8} s 10^1 s 10^4 s $>10^6$ s

molecular dynamics

kinetic Monte Carlo

finite element

ab initio

MD dislocation dynamics

reaction rate theory, phase field

3D dislocation dynamics

Methods

10^{-9} m 10^{-7} m 10^{-6} m $>10^{-3}$ m

Goal of multiscale modeling is fully predictive capability, but: "Prediction is very difficult, especially if it's about the future." ... Niels Bohr

ornl

R. E. Stoller, ORNL.

UT-BATTELLE   *D0000998* 4

Provide four brief examples from various aspects of the multiscale modeling scheme

- primary damage formation, molecular dynamics and kinetic Monte Carlo
- *ab initio* (VASP), accounting for He defects in iron, influence on defect properties and interatomic potential
- atomistic simulation of dislocation-defect interactions, molecular dynamics
- mesoscale (reaction rate theory) model of microstructural evolution
  - illustrate loose (parameter passing) multiscale modeling

ornl

R. E. Stoller, ORNL

ornl

Aspects of Primary Radiation Damage Source Term

(1) associated with fission or fusion reactions in reactors

- "fission fragments", heavy charged particles recoiling from fission event
  - peaks around atomic masses 90 and 140
  - energy ~ 80-100 MeV
  - limited range, primarily impacts fuel
- high energy neutrons (flux >0.1 or >1.0 MeV traditionally used as correlation parameters by nuclear industry)
  - fission spectrum up to ~20 MeV, peak at ~0.65 MeV, $\phi(peak)/\phi(10\ MeV)\sim350$
  - DT fusion at 14.1 MeV
  - displacement cross section minimum at ~1 keV (elastic scattering limit) for iron
- thermal neutrons
  - typically E<0.5 eV, kT_{room} =0.025eV)
  - produce low energy recoils from (n,γ) capture reactions; a few 100s eV in steels

ornl

R. E. Stoller, ORNL

Primary Radiation Damage, con't.

- high energy (up to a few MeV) electrons
  - primarily produced by Compton scattering of fission gamma rays, some from (n,γ) reactions
  - generate low energy recoils (similar to thermal neutrons) by elastic scattering
- nuclear transmutation products
  - gases: primarily hydrogen and helium from (n,p) and (n,α) reactions
  - solid: (n,p), (n,α), $(n,2n)$, (n,γ) with subsequent β decay
  - both thermal and high energy neutron reactions contribute
  - appm to atom-% levels, generally not too significant, but e.g. silicon production in aluminum where $\phi_{th}=2.5\times10^{26}$ n/m^2 (~6 months in HFIR) converts 1% of Al to Si

ornl

MD simulation of primary damage formation

Classical molecular dynamics, typical implementations:

- constant pressure, periodic boundary condition

- boundary atoms not damped, results in some heating

- no electronic losses or electron-phonon coupling, energy of cascade simulation, hence for: T_{dam} = kinetic energy lost in elastic collisions,

$$E_{MD} \sim T_{dam} \, (NRT) < E_{PKA}$$

Range of interatomic potentials have been employed, from simple pair potentials to embedded atom or Finnis-Sinclair, limited work with higher order potentials

- results presented here for modified version of Finnis-Sinclair iron

- can be compared with simple standard model for number of defects produced:

$$\nu_{NRT} = \frac{0.8 \cdot T_{dam}}{2 \cdot E_d}$$

ornl

R. E. Stoller, ORNL.

In contrast to linear damage energy dependence of NRT model, three well defined energy regimes appear

- at lowest energies true "cascade-like" behavior does not occur
- above ~10 keV, subcascade formation dominates
- nearly linear energy-dependence is observed at higher energies, consistent with simple reasoning of K-P or NRT models
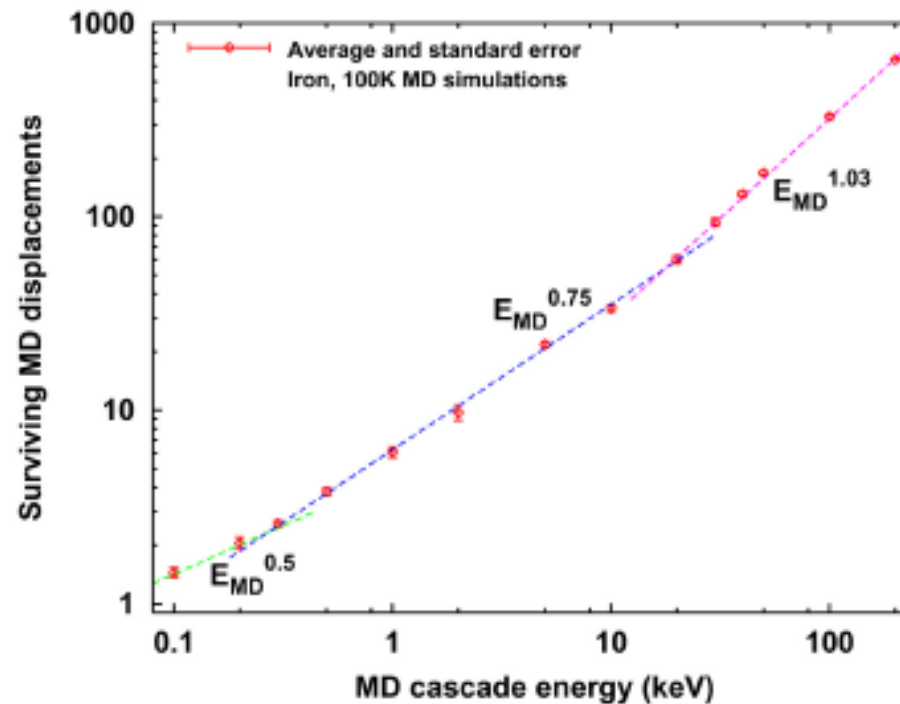
50 keV example

Partial Fe Cascade Database at 100K

MD Cascade Energy (keV)	Corresponding neutron energy (MeV)	Number of Simulations	Typical simulation cell size (atoms)
0.1	0.003351	40	3,456
0.2	0.006818	32	6,750
0.5	0.01749	20	16k/54k
1.0	0.03578	12	54k
2.0	0.07342	10	54k
5.0	0.1911	9	128k
10.	0.3968	15	125k/250k
20.	0.8321	10	250k
50.	2.277	9	2.249M
100.	5.085	10	5.030M
200.	12.31	3	9.826M

ornl

Illustration of subcascade structure at peak damage condition for 5, 10, and 100 keV cascades at 100K
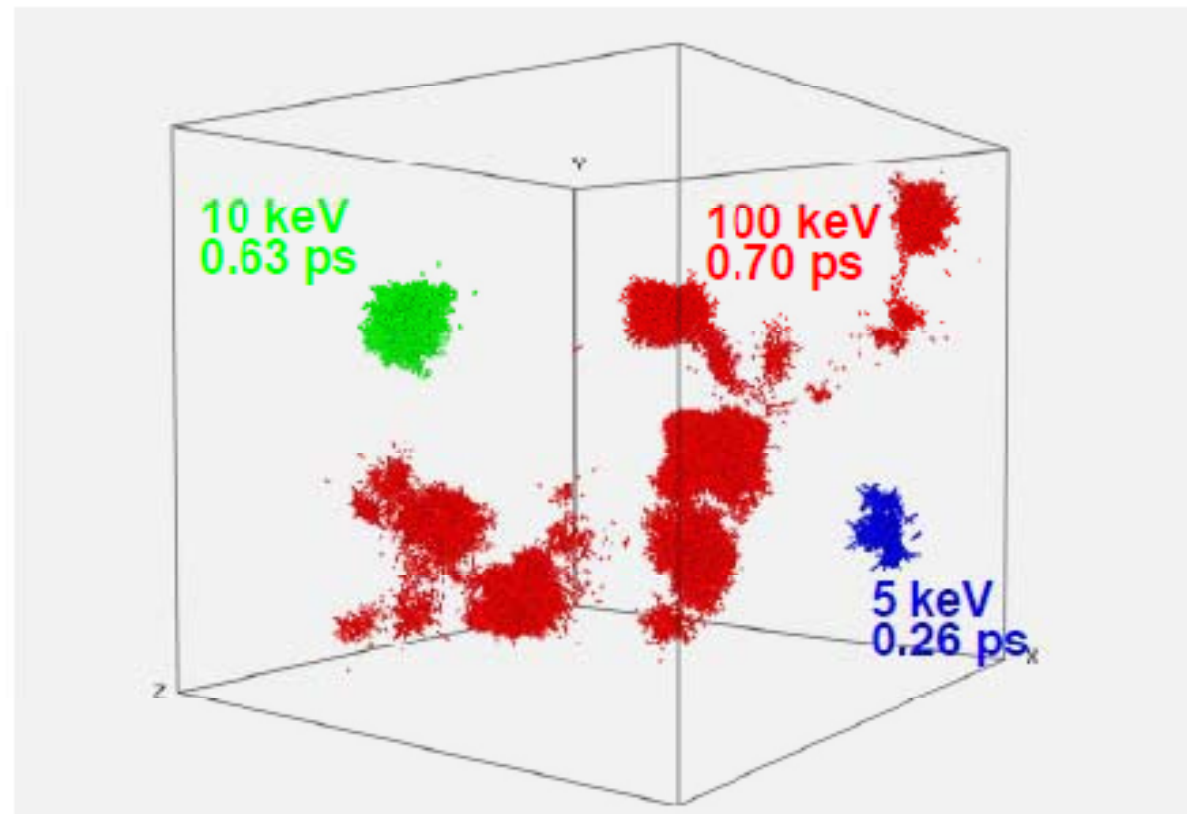
- high energy cascades look like multiple lower energy events, leads to asymptotic behavior with energy
- low energy events between subcascades have higher efficiency

R. E. Stoller, ORNL

Comparison of MD Displacement Cascades in Iron at 100K - Time of Peak Damage

10 keV

100 keV

5 keV

5 keV – 0.26 ps
10 keV – 0.63 ps
100 keV – 0.70 ps

5 nm
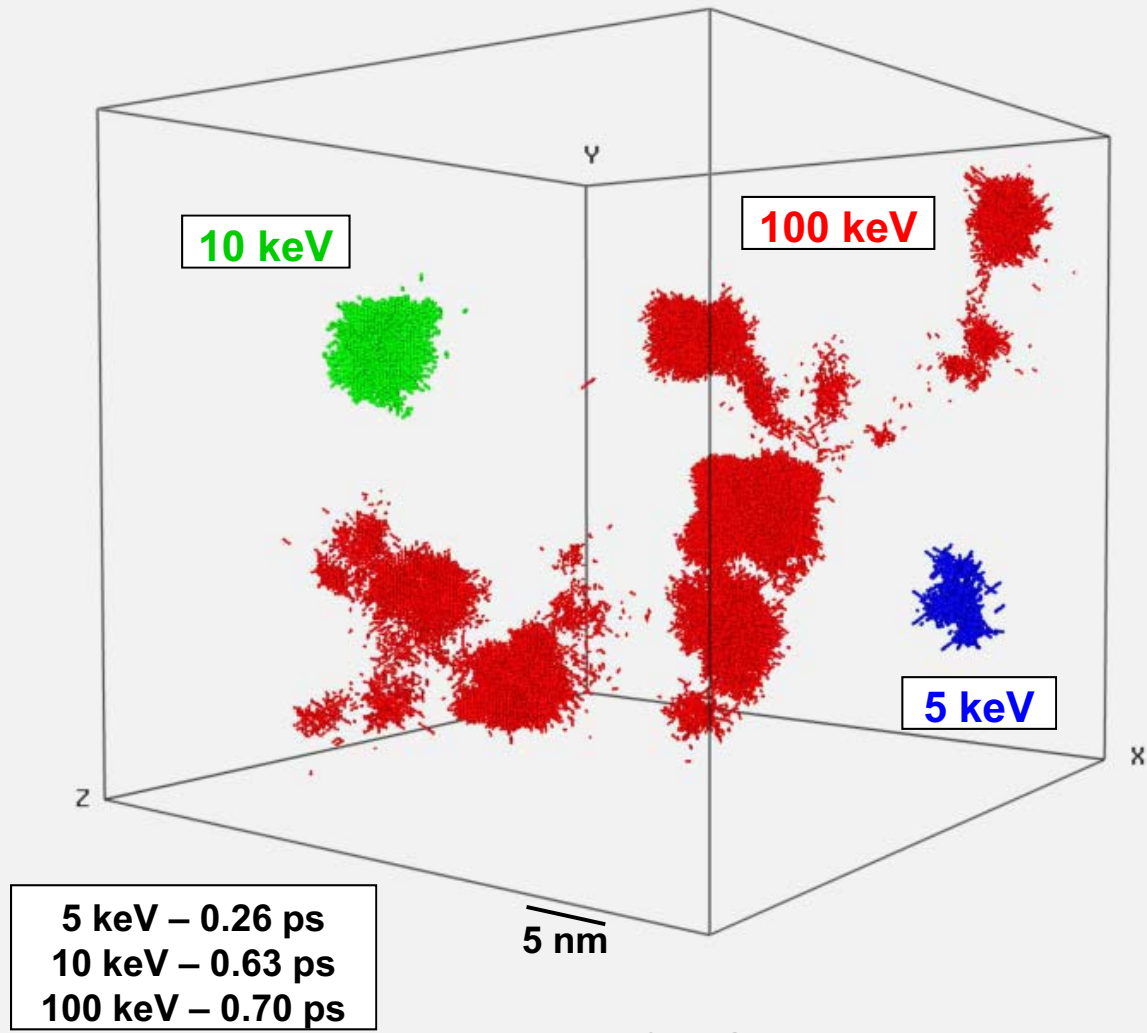
After Stoller

Status of Primary Radiation Damage Simulation

- extensive MD cascade studies have been carried out, largest database for Finnis-Sinclarium "iron

- analysis of the simulations has lead to a good mean description of the dependence on temperature and cascade energy up to fusion-relevant energies

- some anticipated and new phenomena have been revealed and explained: subcascade formation, glissile interstitial cluster formation, 3D and planar channeling effect

Needs

- many more simulations needed to determine influence of 'rare' events

- longer times to be explored in cascade aging studies using KMC

- potential need for more realistic potentials for transition metals such as iron to account for partially-filled d-bands (directional effects) and magnetism

- realistic potentials for multicomponent alloys: ~5 major components in most steels plus critical effects of minor solutes and impurities

ornl

R. E. Stoller, ORNL

Applications of MD-based dislocation dynamics

Investigate atomistic details of dislocation-defect interactions, relevant to hardening mechanisms: dislocation loops, voids, SFTs, precipitates

- obtain critical resolved shear stress as a function of dislocation density, defect density and size; influence of temperature and strain rate

- identify mechanisms important in clearing defects and forming defect-free channels, important in flow localization

X - [111]
Y - [1$\bar{1}$0]
Z - [11$\bar{2}$]

ornl
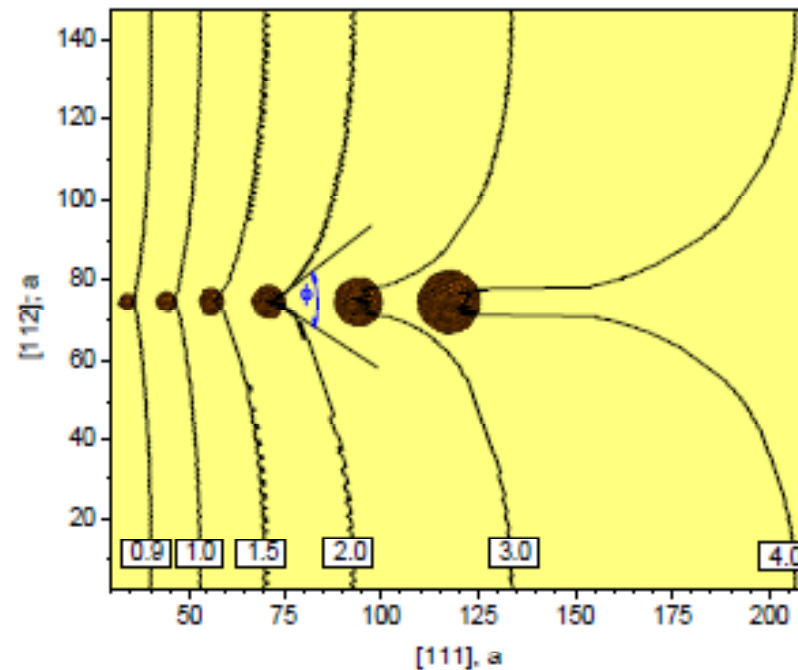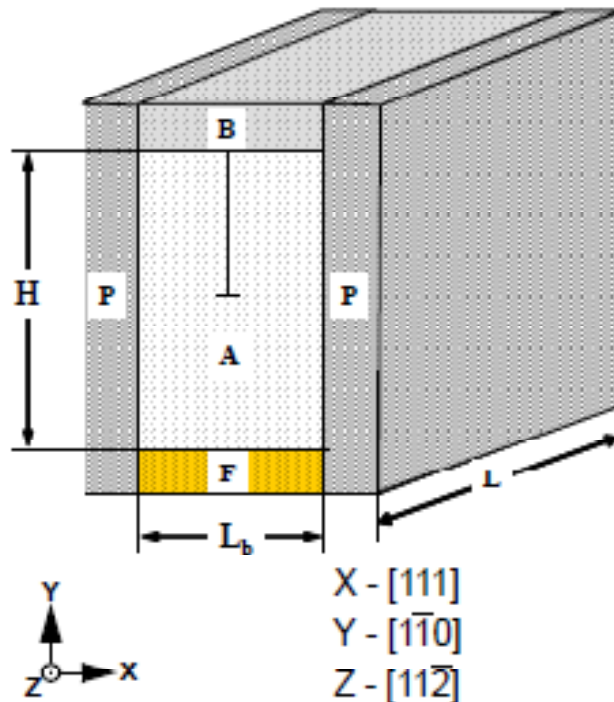
Interaction of Dislocation with Cu Precipitate

R. E. Stoller and Y. Osetsky

Applications

(1) Atomistic nature of dislocation-defect interactions

- radiation-induced increase in yield strength based on simple hardening theory for dispersed barriers

$$\Delta\sigma = T\Delta\tau = T(\alpha Gb) \cdot (\sqrt{Nd})$$

where T is the Taylor factor (3.06), N and d are the radiation-induced defect density and mean diameter, and α is the so-called barrier strength

- values of the barrier strength can be estimated from continuum elasticity calculations and from comparisons between microstructural observations (TEM, APFIM, SANS) and mechanical property changes
- typical values are 0.1 to 1.0, considerable uncertainty associated with superposition rules for multiple defect types, error in microstructural measurements, allowance for invisible defects, etc.
- elasticity-based dislocation models can not account for atomistic details of dislocation-defect interactions

Cu SFT Example-1

ornl

R. E. Stoller, ORNL

Status of MD Dislocation Dynamics

- relevance of atomistic simulations clearly demonstrated, e.g. dislocation-point defect reactions leading to climb, jog formation, etc.; defect destruction, defect creation (single and clusters), effect of free surfaces

- extensive investigations have included edge and screw dislocations in Fe and Cu with obstacles including precipitates (Cu in Fe), SFTs, dislocation loops, and voids, work in progress for multiple defect types and He-filled bubbles

- variables include strain rate (dislocation velocity), temperature, effective dislocation and obstacle densities

Needs

- more and faster cycles to enable more experimentally relevant strain rates, and defect sizes and densities

- hybrid models linking MD up to continuum and down to *ab initio*, Green's function boundary conditions employed in some cases but more work needed

ornl

R. E. Stoller, ORNL.

Application of mesoscale models in radiation effects

- mesoscale models are relevant to many phenomena in materials science and radiation effects
    - grain growth
    - dislocation evolution, by thermo-mechanical or radiation-induced processes
    - void swelling
    - precipitation of additional phases, and solute segregation
    - stress corrosion cracking, and irradiation-assisted SCC
- size scale permits direct comparison with experiments such as TEM and mechanical property measurements
- dependent on fundamental atomistic processes, and controls macroscopic observables such as strength, ductility, creep, ...
- a primary application is the investigation of point defect and solute kinetics and microstructural evolution, so-called mean field models based on reaction rate theory, phase field models and some types of Monte Carlo simulations

ornl

R. E. Stoller, ORNL.

Example from reaction rate theory modeling

starting point is continuity equations describing point defect (vacancy, C_v and interstitial, C_i) populations (analogous equations for solutes):

$$\nabla \bullet \left(D_v \nabla C_v + \frac{D_v C_v}{kT} \nabla U_v \right) + G_v - \alpha C_i C_v - D_v C_v S_v^T = \frac{\partial C_v}{\partial t}$$

$$\nabla \bullet \left(D_i \nabla C_i + \frac{D_i C_i}{kT} \nabla U_i \right) + G_i - \alpha C_i C_v - D_i C_i S_i^T = \frac{\partial C_i}{\partial t}$$

where the ∇ denote spatial derivatives.

- first term on the LHS describes point defect drift to discrete sinks, the $U_{i,v}$ are interaction energies between the point defects and discrete sinks
- $G_{i,v} = \eta G_{dpa} + G_{i,v}^{em}$ is the total point defect generation rate, including thermal emission from sinks, and the $D_{i,v}$ are the point defect diffusivities
- $S_{i,v}^T$ are the total sink strengths for continuum sinks (e.g. cavities, dislocation, grain boundaries, etc.), recombination rate coefficient is given in terms of an effective recombination radius, r_r: $\alpha = 4\pi r_r (D_v + D_i)$

ornl

ornl

- typical assumptions/simplifications
  - the material is treated as a spatially-homogeneous effective medium with embedded effective sinks and sources for point defects
  - spatially-averaged point defect generation rates are also generally employed
  - these assumptions have been relaxed in particular cases, e.g. to investigate cascade-induced fluctuations in point defect concentrations
  - the models are formulated as a series of differential equations describing the production and fate of point defects and the corresponding evolution of the microstructure
- With these approximations, and assuming that the irradiation produces only monomers, the time-dependent or steady state point defect concentrations can be obtained as a solution to the following equations:

$$\frac{dC_{i,v}}{dt} = \langle \eta G_{dpa} + G_{i,v}^{em} \rangle - \alpha C_i C_v - D_{i,v} C_{i,v} S_{i,v}^T$$

Time dependent solution of simple point defect equations

- much different time constants for vacancies and interstitials due to much slower vacancy migration
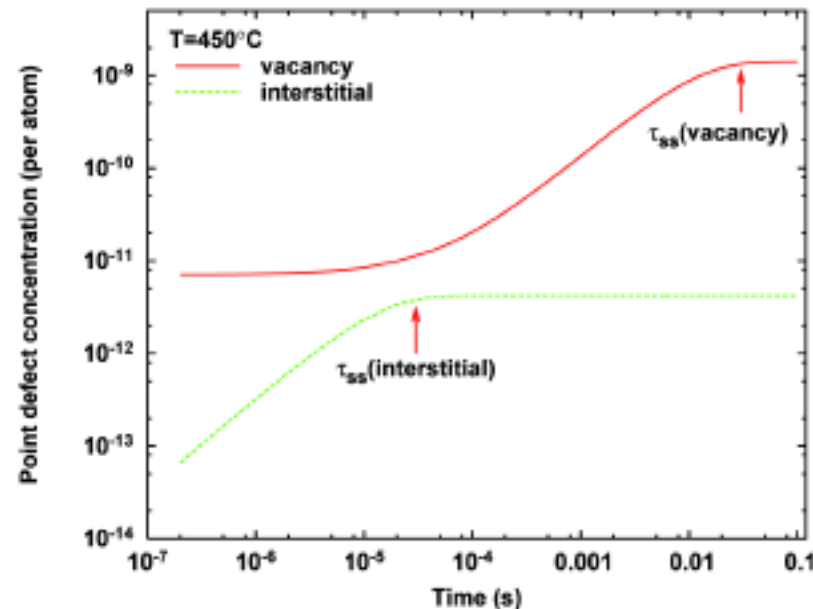
- a minor multiscale problem within a mesoscale method, requires good ODE solver for stiff systems

ornl

However, the success of these models in fitting data can be deceiving (the devil is in the details ...)

- data fitting with incomplete models leads to use of "effective" parameter values, use of parameter-rich models limits confidence in model extrapolation

- for example, if point defect absorption dominated by dislocations with sink strength S_d, swelling rate is proportional to product of η and net dislocation bias $(Z_i^d - 1)$:

$$\frac{dV}{dt} = \frac{\eta G_{dpa}}{S_v^d}\left(Z_i^d - 1\right)$$

- In this case, data fitting can not be used to obtain unique set of model parameters. MD cascade simulations provide independent estimate of η and thereby permit better estimate of Z_i^d.

ornl

R. E. Stoller, ORNL.

- *ab initio* methods and MD can provide improved estimates of material parameters, e.g. point defect formation energies, primary radiation damage parameters

    - former is largely limited to simple materials and small atomic systems, providing limited information on diffusion and defect formation energies, and latter is limited by range of materials for which adequate interatomic potentials can be developed

- most importantly, keep in mind that models are inherently incomplete, sometimes we know what we don't know, sometimes we don't, e.g.:

    - solute effects (alloy thermodynamics) not accounted for in most rate theory models

    - real materials are not spatially homogeneous (see examples above)

    - from MD: neutron irradiation produces small point defect clusters as well as the monomers, ~10-60% defects in clusters, vacancy and interstitial clustering fractions different

    - from MD: observed diffusion behavior more complex than simple 3D, small clusters also mobile, alternate diffusion mechanisms change reaction kinetics (sink strengths of extended defects)

ornl

Summary

Substantial progress in understanding and predicting the behavior of materials has been provided by theory and computational modeling

Further progress requires additional research in the following areas:

- Electronic structure calculations to obtain intrinsic and defect properties in iron and its alloys, including the effects of He and H

- Computationally-efficient, physically-robust interatomic potentials for multicomponent alloys, including effects of directional bonding and magnetism

- Advanced atomistic and mesoscopic models describing the many defects and processes that interact in complex ways in multicomponent, multiphase materials

- Linked and multiscale (atomistic, mesoscopic, and continuum) deformation and fracture models for predicting hardening, plastic instability, changes in ductile-to-brittle fracture, dimensional instability, and creep/creep rupture behavior under realistic loading conditions

ornl

ornl

UT-BATTELLE *D0000998* 24

Atom Probe Tomography and Small Angle Neutron Scattering Are Used to Reveal Mechanisms of Irradiation Embrittlement –Atomistic Modeling is Used to Help Develop Kinetic Embrittlement Models

Irradiatio et Frango ut Patefacium – I Irradiate and Break In Order To Reveal

20 keV

40 keV

10 keV
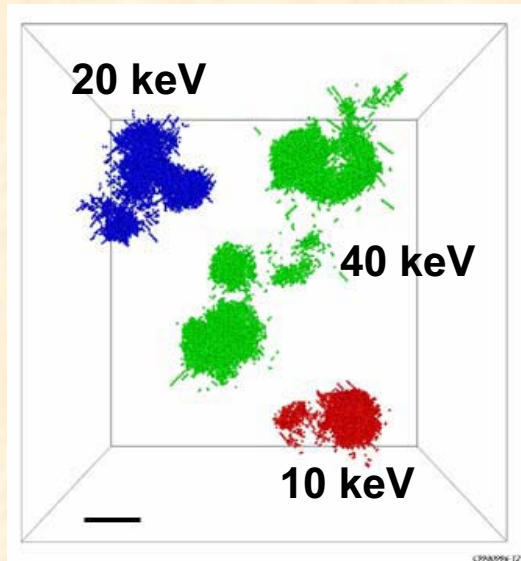
Neutron radiation produces an extremely high number density of nanoscale copper-, manganese-, nickel-, silicon-, and phosphorus-enriched precipitates.
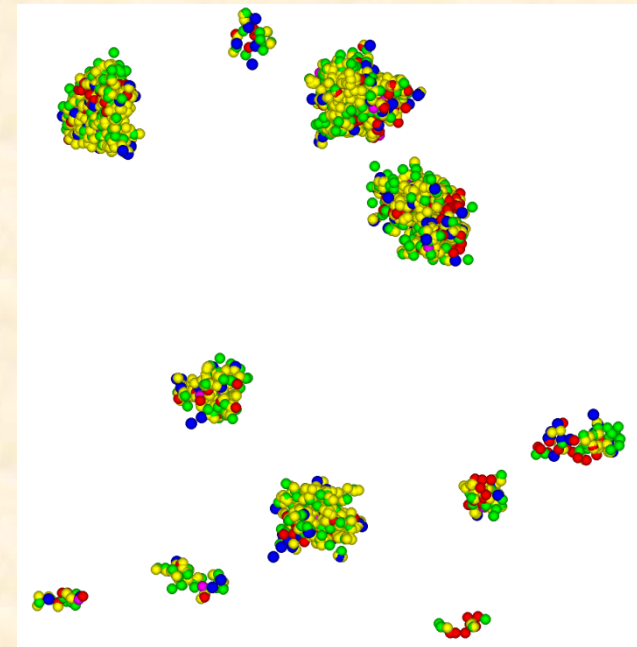
Fe Cu Ni Mn Si P atoms
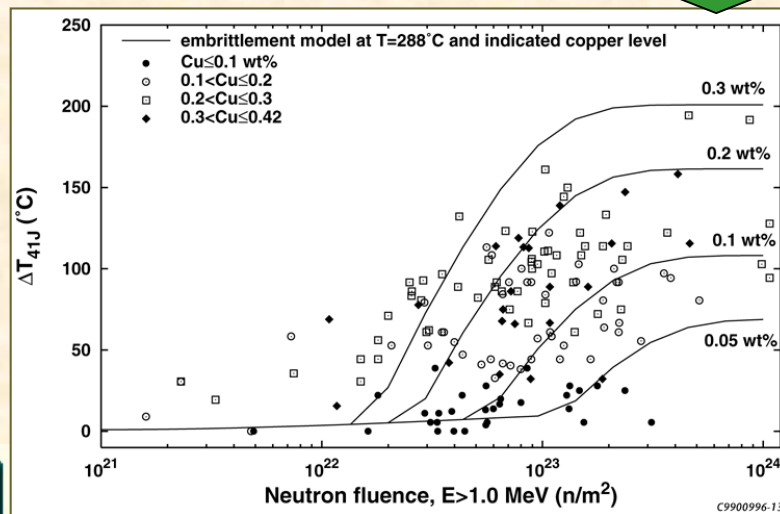
Combination of experimental, modeling, and microstructural studies leads to advances in predictive capability.

Both VVER-1000 Materials and Palisades Weld are High Nickel, but Only Palisades has High Copper

Two different types of high nickel pressure vessel steels with low and high copper contents were selected for this study.

Element		VVER 1000 reactor base		weld			Palisades reactor weld	
		wt.%	at. %	wt. %	at. %		wt.%	at. %
Cu ⟶	Low	0.05	0.04	0.07	0.06	High	0.20	0.18 High
Ni ⟶	High	1.26	1.19	1.78	1.69	High	1.20*	1.14 High
Mn ⟶		0.46	0.46	0.80	0.81		1.27	1.29
Si ⟶		0.30	0.59	0.33	0.65		0.18	0.36
Cr		2.2	2.34	1.80	1.93		0.04	0.04
Mo		0.51	0.30	0.59	0.33		0.55	0.32
V		0.10	0.11	-	-		0.003	0.003
C		0.17	0.78	0.06	0.28		0.11	0.51
P		0.008	0.014	0.005	0.009		0.014	0.03

*Nickel level limit of Reg. Guide 1.99 Rev. 2

VVER-1000 Fluences (E > 0.5 MeV)
Base   2.4, 9.4 and 14.9 × 10^{23} m^{-2}
Welds   2.4, 5.2, 6.4 and 11.6 × 10^{23} m^{-2}
PIA
2 and 24 h at 450°C
Palisades Weld Fluence : 2.4 x 10^{23} m^{-2}

Atom Probe Tomography is Performed by Evaporating Atoms from Tip of a Needle and Subsequent Analysis of Composition and Position
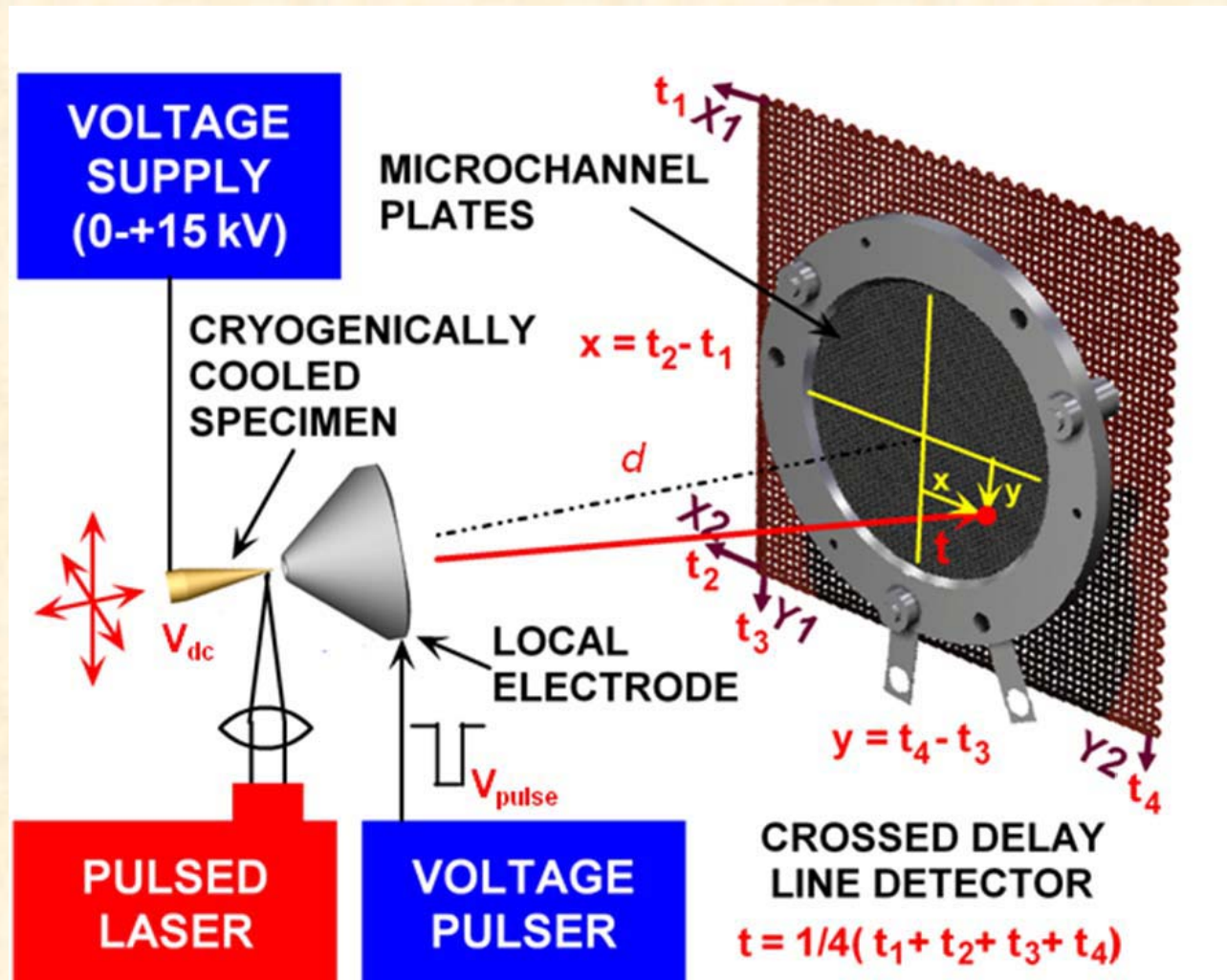
Elemental Segregation to Dislocations in VVER-1000 Weld Metal Was Observed

Weld Metal
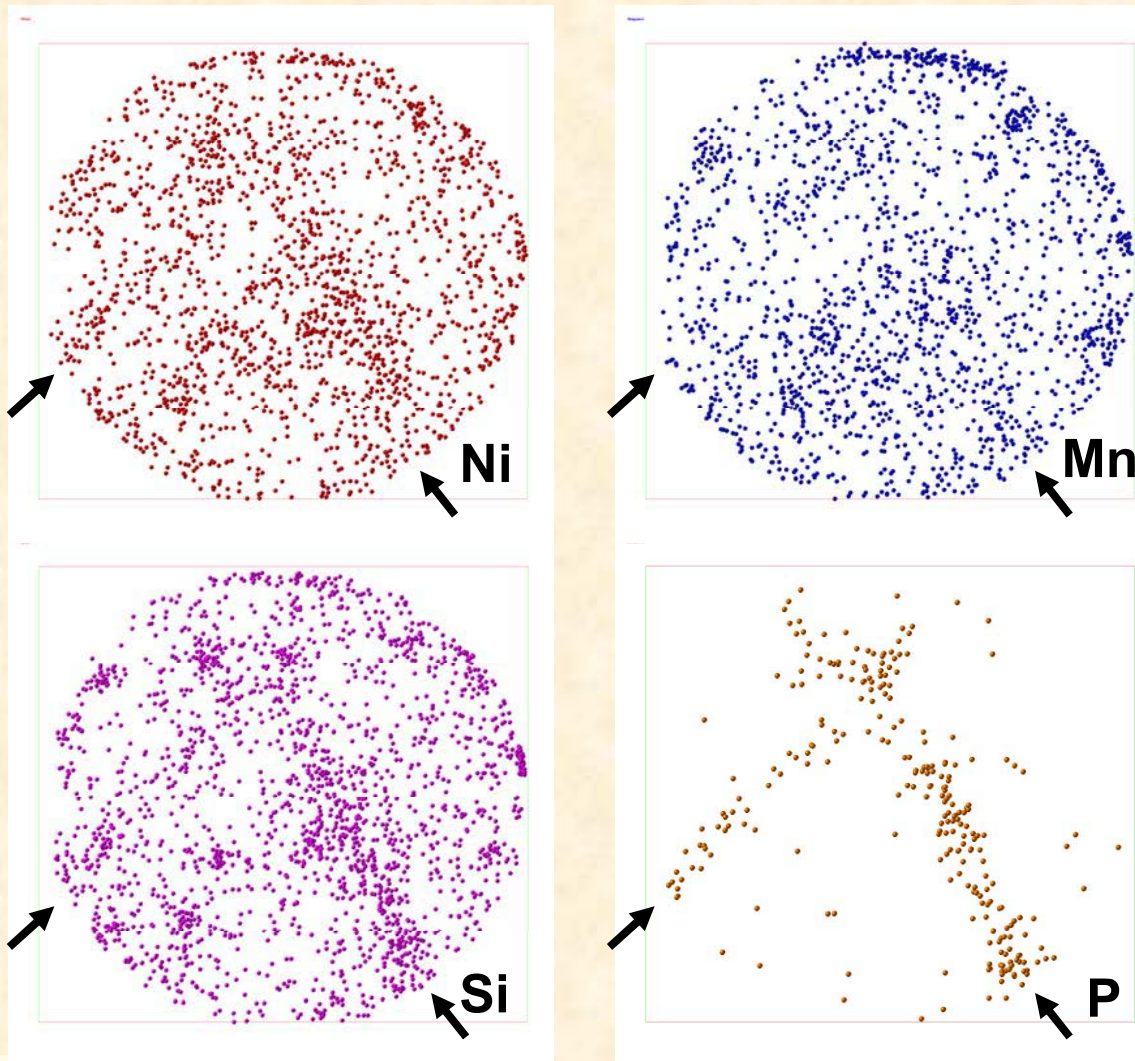
Phosphorus, nickel, silicon and to a lesser extent manganese were found to be segregated to the dislocations.

dislocation →

P   **Ni**
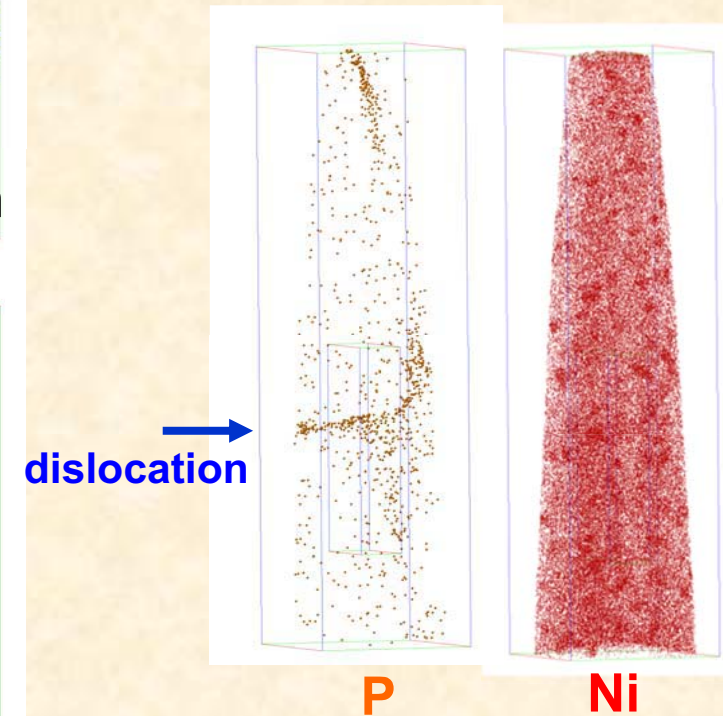
Fluence 11.5 × 10^{23} m^{-2}

Palisades A533B Weld Exhibited a ΔT_{41J} (102°C) Less Than the Reg. Guide 1.99 Rev. 2 Prediction (154°C).

$T_i = 288°C, \quad \Phi = 1.4 \times 10^{19}$ n/cm^2 (>1 MeV)

Palisades weld: 0.2 wt% Cu 1.2% Ni

Unirradiated
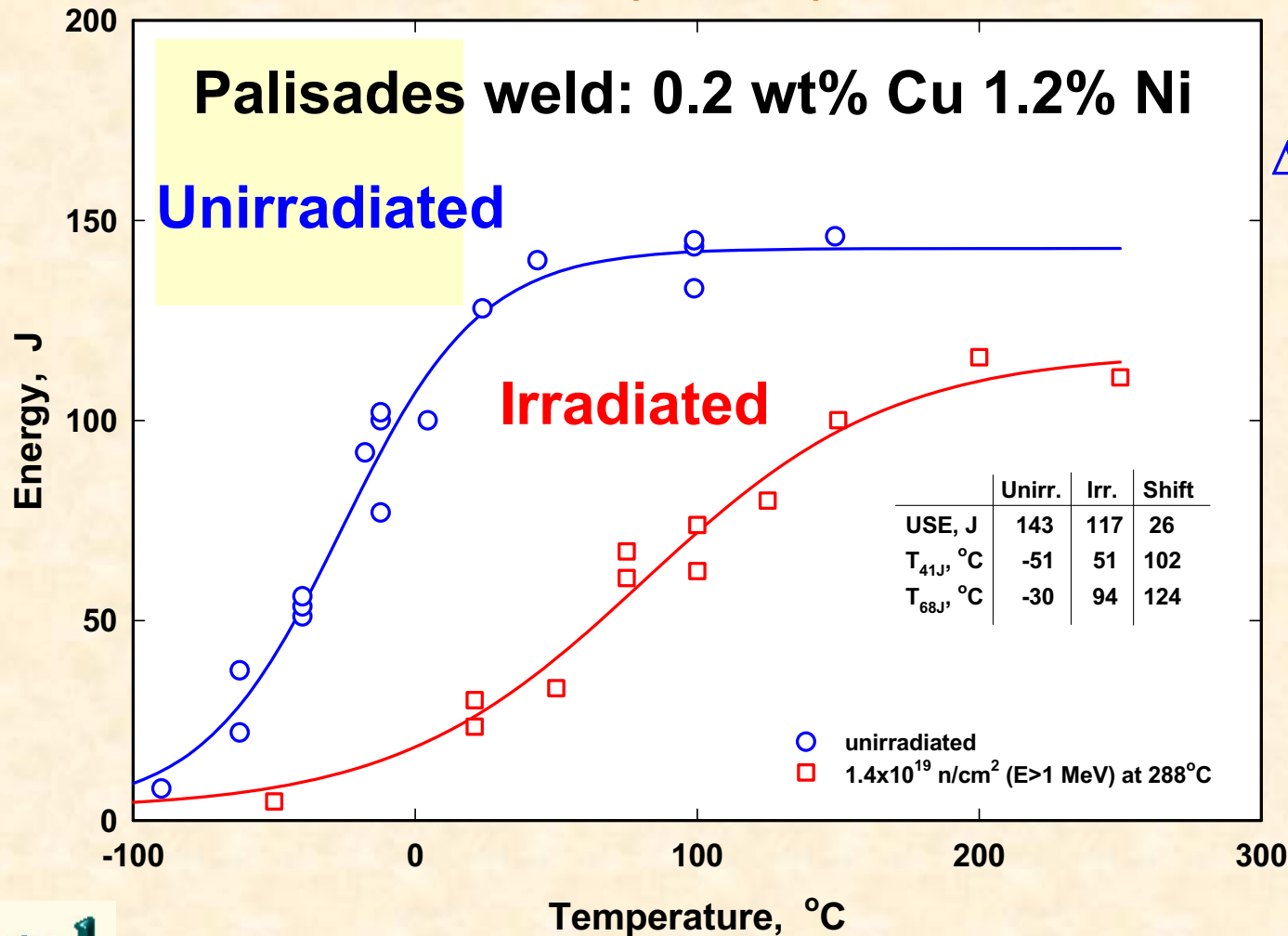
Irradiated

$\Delta T_{41J} = 102°C$

RG1.99-2=154°C

EWO=137°C

E900=137°C

	Unirr.	Irr.	Shift
USE, J	143	117	26
T_{41J}, °C	-51	51	102
T_{68J}, °C	-30	94	124

○ unirradiated
□ 1.4x10^{19} n/cm^2 (E>1 MeV) at 288°C

Energy, J

Temperature, °C

High Number Density of Precipitates Observed in Irradiated Palisades Weld
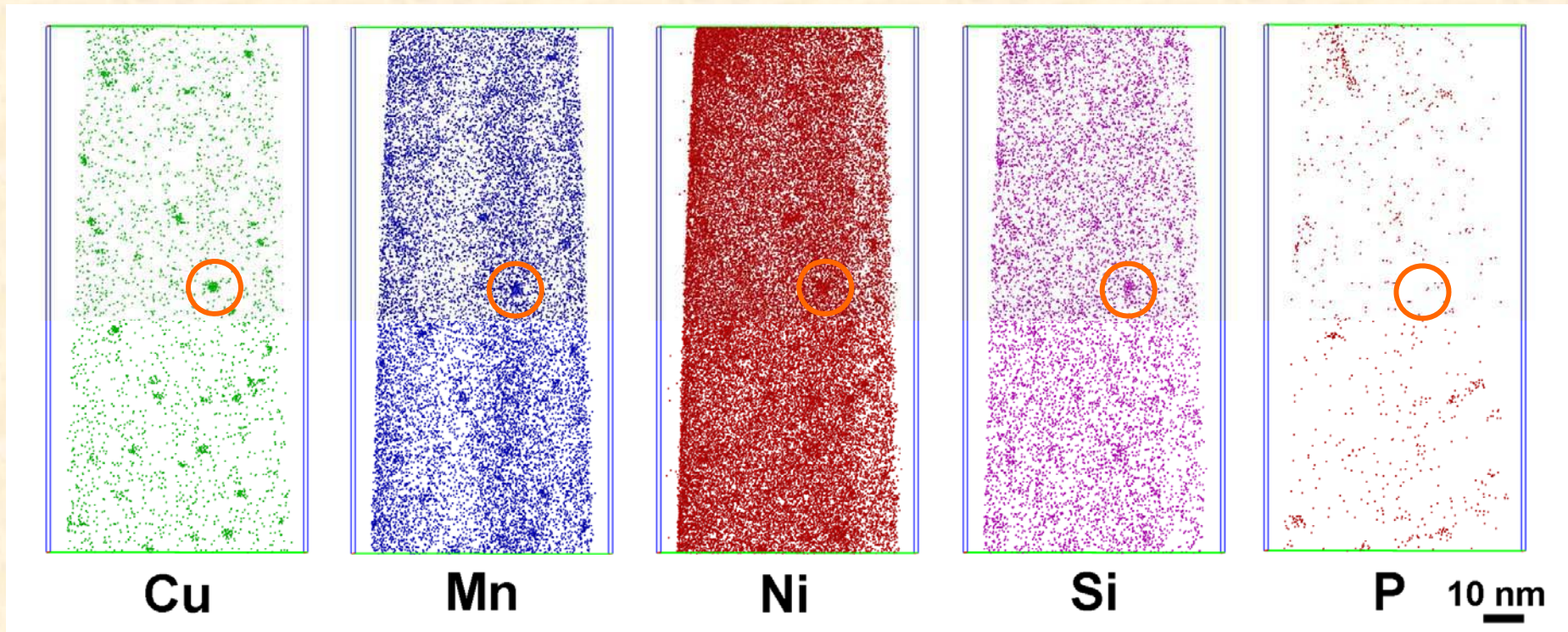
| Cu | Mn | Ni | Si | P | 10 nm |

A high number density of Cu-, Mn-, Ni-, Si- and P-enriched precipitates were observed in the neutron irradiated weld.

	Cu	Mn	Ni	Si	P
N_v = 5 x 10^{23} m^{-3}	87.0	0.42	0.77	0.23	0.15 at. %

r_G = 1.1 nm   Number of atoms in precipitate = 30.

Matrix Copper = 0.07 at. %

Fluence:1.4 x 10^{19} cm^{-2} (>1 MeV)

APT Reveals Cu and P Segregation to Dislocation in Palisades Weld

Cu P
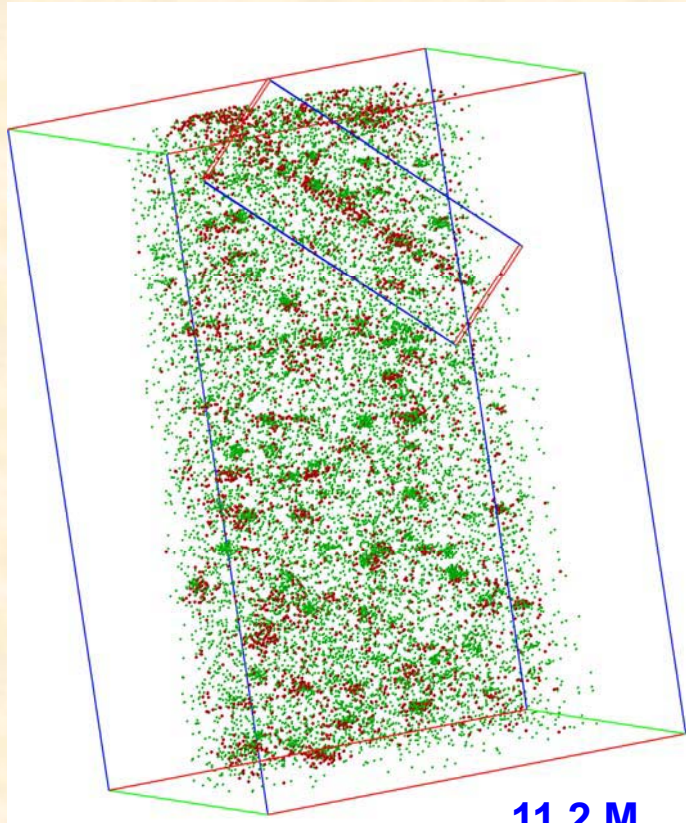
11.2 M atoms

10 nm

**Neutron irradiated Palisades weld =1.4 x 10^{19} n cm^{-2} (E >1 MeV)
Temperature = 288°C.**
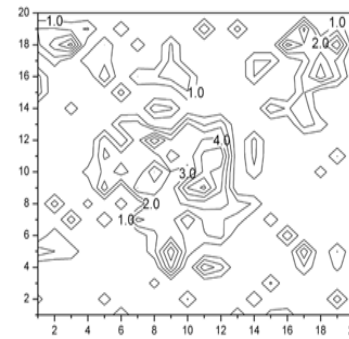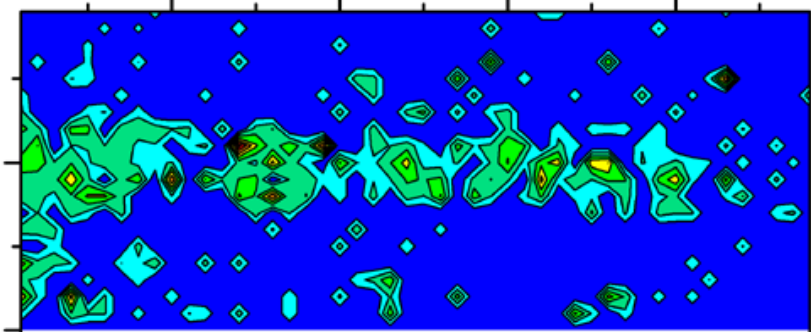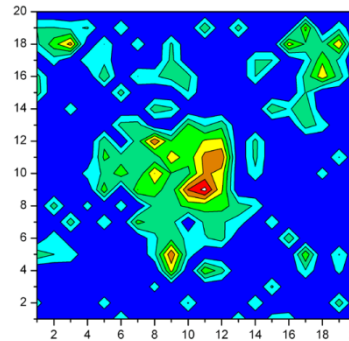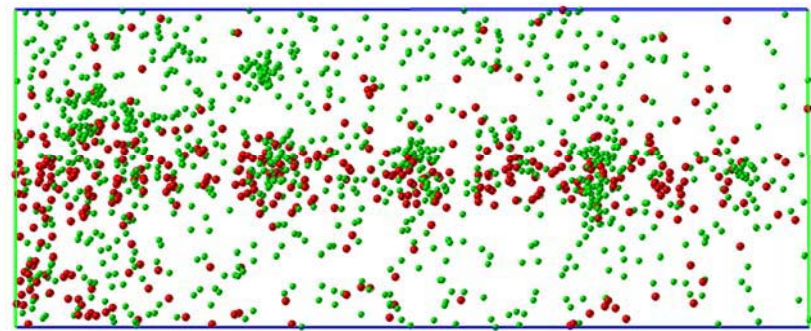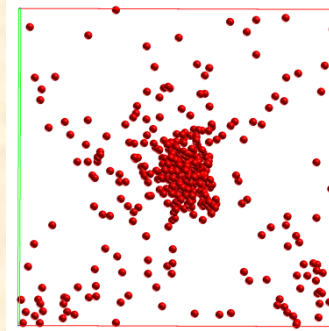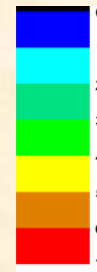
- Tracer method indicates levels of 3-4 at% P with peaks of up to ~7% P at the dislocation.
- The extent of the phosphorus segregation was ~5 nm.

Summary of Atom Probe Tomography Comparisons for VVER-1000 and PWR RPV Steels

- **For the low-Cu VVER-1000 materials, higher Ni content leads to higher embrittlement for a given fluence.**
  - **Low number density of ultrafine Ni-, and Mn-enriched precipitates observed (even though low Mn material), but higher fluence is required for high embrittlement.**

- **There is a reasonable correlation between ΔT_{41} and ΔYS vs number density of Ni-, Si-, and Mn-enriched nanoclusters.**

- **For the Palisades material with 0.2Cu and with Ni similar to VVER-1000 base material, ultrafine Cu-, Mn-, and Ni-enriched precipitates were observed, but at much lower fluence than for VVER-1000.**

- **High-Cu, high-Ni KS-01 weld exhibited a high number density of Cu-, Mn-, Ni-, P-, and Si-enriched precipitates even at relatively low fluence (0.8E19).**

- **Mn exists in all the irradiation-induced precipitates, even when the level is quite low, as in the VVER-1000 base metal (0.46 wt%).**

- **Phosphorus and other elemental segregation to dislocations and grain boundaries was also observed.**

Small-Angle Neutron Scattering (SANS) Measurements of Three Hi-Cu Steels Show Thermal Annealing Reduced Precipitate Number Density and Volume Fraction, but Increased the Radius
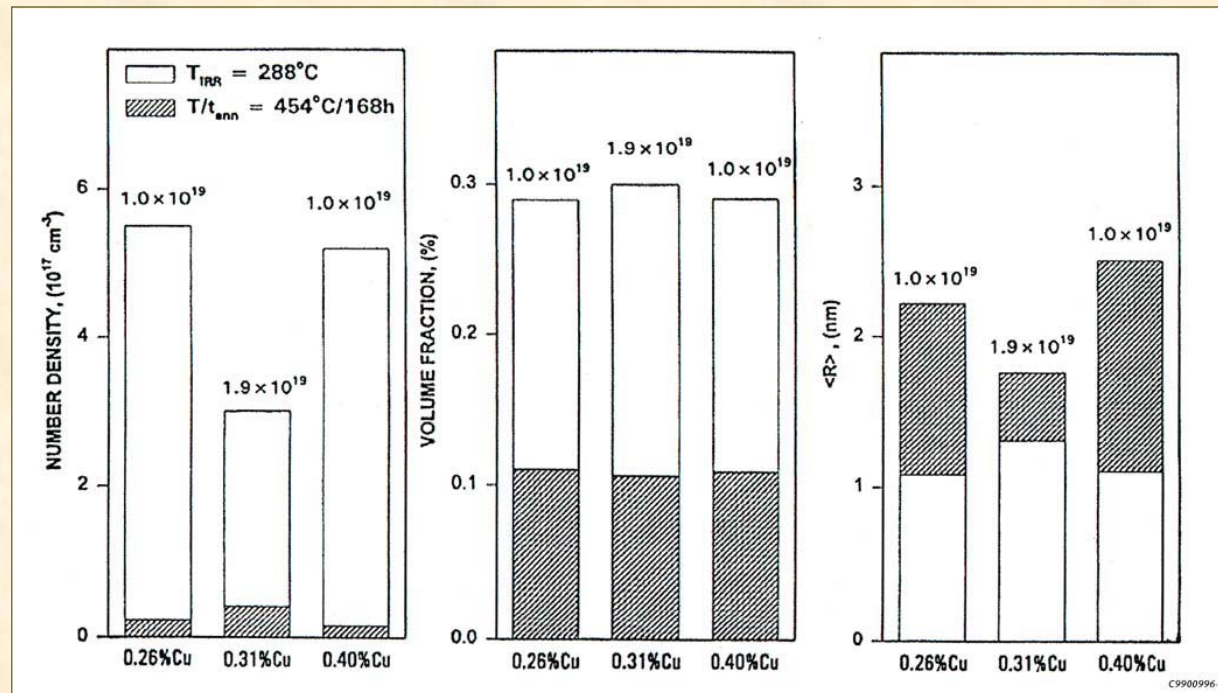
Number density, volume fraction, and the mean radius of scattering centers for three high-copper submerged-arc welds, including HSSI Weld 73W (0.31 wt % Cu) in the irradiated and the irradiated/annealed conditions.

Summary and Conclusions For Late Blooming Phases

- For low Cu & Cu-free steels, Mn-Ni(-Si) LBPs are observed as previously *predicted based on thermodynamic considerations and modeling.*

- Systematic search based on special alloys and irradiations and characterization by a variety of techniques.

- LBPs and large $\Delta\sigma_y$ recently verified in Cu-free steels - although even small amounts of Cu play a key role.

- Key issues - combined effects of T_i, Ni, Mn, Cu, ϕ and Φ.

- Models can be fine tuned and used to guide experiments.

- Experiments underway (e.g., long term annealing of specimens to probe MNP phase boundaries) but material is very limited and *irradiation facilities have disappeared.*

- Studies of high fluence low flux surveillance materials very useful .

- *However additional well designed irradiation experiments are critical!!!!!!!!!*

After Odette and Miller